Asociación Argentina
de Mecánica Computacional

Mecánica Computacional Vol XXVII, págs. 899-907 (artículo completo)
Alberto Cardona, Mario Storti, Carlos Zuppa. (Eds.)
San Luis, Argentina, 10-13 Noviembre 2008

INVESTIGATION OF THE EFFECT OF CUBE TEXTURE ON FORMABILITY OF FACE CENTER CUBIC SHEET METALS

María A. Bertinetti, Pablo A. Turner and Javier W. Signorelli

Instituto de Física Rosario, (IFIR-CONICET), Universidad Nacional de Rosario, Bv. 27 de Febrero 210bis, 2000 Rosario, Argentina, signorel@ifir.edu.ar, http://www.ifir.edu.ar/

Keywords: Formability, Cube texture, Cristal Plasticity.

Abstract. Cube texture component is inevitably present in face center cubic sheet metal. Such preferred orientation leads to anisotropic properties which affect the sheet formability. In this research, the effect of the cube texture on forming-limit strains is studied using a rate-dependent viscoplastic law in conjunction with the Marciniak-Kuczynski approach. The forming limit diagram and yield locus are determined for several spreading of grain orientations around the ideal {100} <001> component. The spreading respect to the ideal orientation is taken assuming a uniform distribution with a standard deviation or cut-off angle from 0 degrees to 15 degrees. The trend of the predicted limit strains shows that the main differences in the forming limit strains have a correlation with the sharpness of the yield locus near equi-biaxial stretching path, and also with the texture evolution and subsequent selected slip systems predicted by each model.

1 INTRODUCTION

It is known that one of the principal factors affecting the formability and the macroscopic anisotropy of polycrystalline sheet metals is the crystallographic texture. In rolled Face Center Cubic (FCC) sheets, crystallographic textures are frequently classified in terms of the rolling and recrystallization ideal components. Many research works have been carried out to assess the influence of these typical texture components on the forming limit strains (Barlat and Richmond, 1987; Zhou and Neale, 1995; Wen et al., 2005) and on the macroscopic anisotropy. Recently, Wu et al. (2004) and Yoshida et al. (2007), based on a generalized Taylor-type polycrystal model, or Full Constraint (FC) model, analyzed the effect of the texture components on the initiation of localized necking in FCC materials in conjunction with Marciniak-Kuczynski (M-K) technique (Marciniak and Kuczynski, 1967). Particularly, Wu performed a detailed study of the influence of the cube orientations on sheet metal formability. They calculated the limit strains for different widespread (ideal, 3°, 7°, 11° and 15°) around the ideal {100}<001> orientation and found, unexpectedly, that the calculated Forming Limit Diagrams (FLD) of cube (11º) and cube (15º) are significantly higher than that of the random texture near biaxial stretching. They claimed that this behavior could be correlated to the sharpness of the yield locus at the equi-biaxial state. This result was also reported by Qiu et al. (1995). Likewise, the same observation was done by Yoshida, who found that only the cube texture component yields limit strains higher than that for a random texture in the biaxial stretch zone.

Forming limit simulations are sensitive to the material constitutive model. In this paper we review the results discussed by Wu et al. (2004) about the effect of the cube texture on the sheet formability, but using a Viscoplastic Self-Consistent polycrystalline formulation (VPSC) plus the Marciniak-Kuczynski approach, which is going to be referred as MK-VPSC from here on (Signorelli et al., 2008). It is shown that the simulations carried out in this framework give the expected results when limit strains are calculated from ideal cube to the random texture, overcoming the results reported using MK-Taylor approaches.

2 MK-VPSC APPROACH

In order to simulate the material response, fully accounting for its heterogeneity and anisotropy, a rate-dependent polycrystalline model is employed. As initially proposed by Molinari et al. (1987), the model starts from the viscoplastic (VP) behavior of single crystals and uses a self-consistent (SC) homogenization scheme for the transition to polycrystals (VPSC). Unlike the FC model, for which the local strains in the grains are considered to be equal to the macroscopic strain applied to the polycrystal, the SC formulation allows each grain to deform differently, according to its directional properties and the strength of the interaction between the grain and its surroundings. In this sense, each grain is in turn considered as an ellipsoidal inclusion surrounded by a Homogeneous Effective Medium (HEM) that has the average properties of the polycrystal. The interaction between the inclusion and the HEM is solved by means of the Eshelby's formalism (Mura, 1988). The properties of the HEM are not known in advance because they result from an average of the individual grains behavior, once convergence is achieved. Here, we present the main equations of the VPSC model. An exhaustive presentation and discussion of the VPSC formulation can be found in Lebensohn and Tomé (1993).

The deviatoric part of the viscoplastic constitutive equation of the material phase at a local level is described by means of the nonlinear rate-sensitivity law, which can be written in a pseudo-linear form, defining a single-crystal, viscoplastic secant modulus $\mathbf{M}$:

$$\mathbf{d} = \mathbf{M} : \mathbf{s} \tag{1}$$

where $\mathbf{M}$ is a function of the Schmid tensor $\mathbf{m}^s$ (which describes the geometry of the s slip system in the single crystal), γ_0 is the slip plane's reference strain rate, τ_c^s is the initial critical shear stress and m is the rate-sensitivity. The interaction equation relates micro (grain-ellipsoid) and macro (polycrystal-HEM) strain rate $(\mathbf{d},\ \bar{\mathbf{d}})$ differences, with micro and macro deviatoric stress $(\mathbf{s},\ \bar{\mathbf{s}})$ differences:

$$\mathbf{d} - \bar{\mathbf{d}} = -\tilde{\mathbf{M}} \left(\mathbf{s} - \bar{\mathbf{s}} \right) \tag{2}$$

where $\tilde{\mathbf{M}}$ is the interaction tensor, which is a function of the overall modulus and the shape and orientation of the ellipsoid that represents the embedded grain. The macroscopic (overall) secant modulus $\overline{\mathbf{M}}$ can be adjusted iteratively using the following self-consistent equation:

$$\overline{\mathbf{M}} = \left\langle \mathbf{M} : (\mathbf{M} + \tilde{\mathbf{M}})^{-1} : (\overline{\mathbf{M}} + \tilde{\mathbf{M}}) \right\rangle \tag{3}$$

$$\bar{\mathbf{d}} = \overline{\mathbf{M}} : \bar{\mathbf{s}} \tag{4}$$

where $\langle\ \rangle$ denotes a weighted average over all the grains in the polycrystal.

In the present study, the strain hardening between slip systems is taken into account by adopting an isotropic hardening scheme. The evolution of the critical shear stresses is given by:

$$\dot{\tau}_c = \sum_s h^s \left| \dot{\gamma}^s \right| \tag{5}$$

where h^s are the hardening moduli behavior which depend on γ (accumulated sum of the single slip contributions to γ^s). These moduli can be written using the initial hardening rate h_0 and the hardening exponent n:

$$h^s = h_0 \left(\frac{h_0 \gamma}{\tau_c^s n} + 1 \right)^{n-1}; \qquad \gamma = \sum_s \int_0^t \left| \dot{\gamma}^s \right| dt \tag{6}$$

The macroscopic values of the strain rates, $\bar{\mathbf{d}}$, and stresses, $\bar{\mathbf{s}}$, are obtained by averaging the local values weighted by the volume fraction of crystal orientations.

The VPSC formulation to model the aggregate behavior is implemented in conjunction with the well-known M-K approach. As it has been originally proposed by Marciniak and Kuczynski, their analysis postulated the existence of a material imperfection such as a groove or a narrow band across the width of the sheet. In its modified form (Hutchinson and Neale, 1978), an angle Ψ with respect to the X_1 reference direction (Figure 1) determines the band's orientation.

The thickness along the minimum section in the band is denoted as $h_b(t)$, with an initial value $h_b(0)$, while an imperfection factor f is given by the initial thickness ratio inside and outside the band:

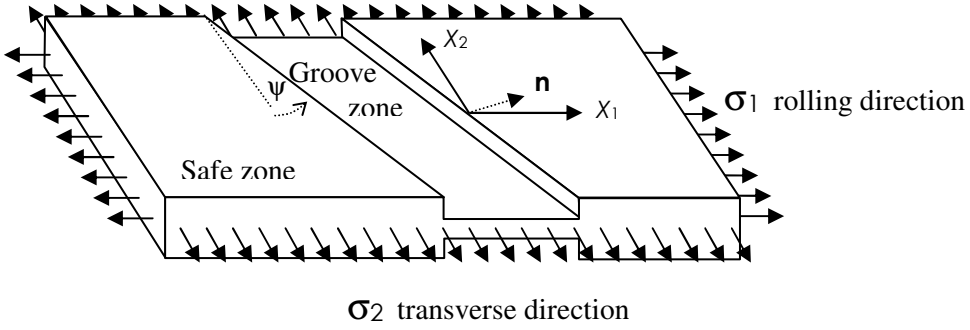

Figure 1: Initial defect approach.

$$f_0 = \frac{h_b(0)}{h(0)} \tag{7}$$

with $h(0)$ being the initial sheet thickness outside the groove.

Equilibrium and compatibility conditions must be fulfilled at the interface with the band. Following the formulation developed by Wu et al. (1997), the compatibility condition at the band interface is given in terms of the differences between the velocity gradients $(\bar{\mathbf{l}}, \bar{\mathbf{l}}^b)$ inside and outside the band respectively:

$$\bar{l}_{ij}^b = \bar{l}_{ij} + \dot{c}_i n_j \tag{8}$$

where n_j are the components of the unit normal to the band, and $\dot{c}_i$ are parameters to be determined (here, and subsequently, the i and j indices are either 1 or 2). The equilibrium conditions required at the band interface are given by

$$n_i \bar{\sigma}_{ij}^b h_b = n_i \bar{\sigma}_{ij} h \tag{9}$$

where $\bar{\boldsymbol{\sigma}}$ denotes the Cauchy stress. The boundary condition $\bar{\sigma}_{33} = 0$ is applied as follows:

$$\bar{\sigma}_{ij} = \bar{s}_{ij} - \bar{s}_{33} \delta_{ij} \tag{10}$$

The system of equations (4), (8), (9) and (10) can be solved to obtain $\dot{c}_i$ by substituting Eq. (4) into the incremental form of Eq. (9), and using Eq. (8) to eliminate the symmetric strain increments $\bar{\mathbf{d}}$ in the band. At any increment of strain along the prescribed strain path, the nonlinear system of two equations is solved. The minimum strain state ε_{11}^*, ε_{22}^* outside the band for various initial inclinations of the groove are defined as forming-limit strains. In the present work, the failure condition is reached when the symmetric part $\bar{d}_{11}^b > 20\,\bar{d}_{11}$.

A detailed discussion of the integration of the polycrystalline model inside and outside the band can be found in Signorelli et al. (2008).

3 RESULTS AND DISCUSSION

The relation between the sheet formability and its initial texture has been already shown in numerous experimental works (Wu et al., 1997; Wu et al., 1998; Knockaert et al., 2002; Viatkina et al., 2005). In order to understand the influence of the different crystal orientations on the FLDs, we investigate the effect of the cube texture in a manner similar to Wu et al.

(2004), but using two interaction models: MK-FC and MK-VPSC. Comparisons of the simulations carried out with these two approaches are presented and discussed below.

To investigate the cube texture effect on the limit strains, we generate a random distribution of orientations and five different "cube textures", each one made up of grains with different orientations dispersed in a certain configuration. The cube orientations belonging to a given "cube texture" are calculated in terms of the number of grains having a misorientation respect to the ideal one lower than a given value. As an example, a "cube 15° texture" is the one with grains presenting a misorientation respect to the ideal cube orientation {100}<001> of less than 15°, uniformly distributed in that area. Figure 2 shows the {111} pole figures for the ideal cube, cube 3°, cube 7°, cube 11° cube 15° and random cases.

For calculations, a polycrystal with 1000 grains is used to simulate the material behavior of FCC sheet metals, for both the homogeneous sheet and the band. It is assumed that the initial textures, the sheet and the band ones, are the same, and that the slip-induced hardening law used in this work is isotropic for all slip systems; the slip reference plastic shearing rate is assumed to be $\dot{\gamma}_0 = 0.001\ s^{-1}$. The initial imperfection value, f_0, is taken to be 0.99 for all computations performed in this work.

To analyze the development of deformation localization during proportional straining, the calculations have been performed for the range $-0.5 \le \rho \le 1$. So, the entire FLD of a sheet is obtained by repeating the procedure for different paths outside the band, as prescribed by the strain ratio ρ, with $\rho = \bar{l}_{22}/\bar{l}_{11} = \bar{d}_{22}/\bar{d}_{11}$. For a real sheet material, numerous initial imperfections exist with different orientations. A usual estimate of a forming limit strain is obtained by calculating the limit strain for various values of the initial band orientation Ψ, and selecting the minimum value as the actual forming limit strain. We have scanned every 5° over the range of Ψ's and then determined the critical groove angle that produces the minimum predicted localization strain.

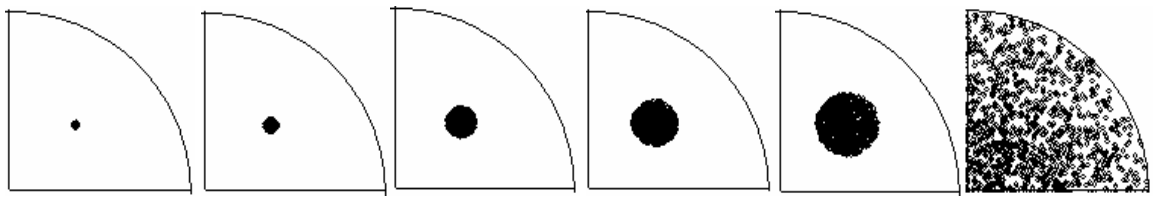

Figure 2: Calculated textures as {111} pole figures for grain orientations with a misorientation respect to the ideal cube orientation of less than the given value.

These different initial textures strongly affected the forming limit curves as plotted in Figure 3. The results are quite similar to those reported by Wu et al. (2004) when the MK-FC approach is used. But the tendency is quite different, particularly in the biaxial stretching, when simulations are carried out with MK-VPSC. The results shown clearly remark the differences between VPSC and FC homogeneization schemes, although their shape and level are similar in the uniaxial range.

No significant differences are found for the ideal and the cube 3°, since for these cases the yield locus are almost the corresponding to the cube single crystal, and both models predict the same shape and tendency. In the negative minor-strain range ($\rho < 0$) of the FLD, the shapes are nearly straight lines with the maximum values at $\rho = -0.5$. For these two textures, and with both models, the FLD curves slope downwards for plane-strain tension to equi-

biaxial stretching, with the minimum strain values at $\rho = 1$, which are far below from those of the random texture. As one expect the larger the spread around the ideal orientation the larger the formability and the limit strains. The calculated FLD of the random texture should be above all of them, and the FLD of a particular spread should be between those of the ideal cube and the random cases. However, when using the MK-FC model, the limit strains for cube 7°, cube 11° and cube 15° are higher than that of the random texture in the biaxial stretching zone (left in Figure 3). The same unexpected behavior has been reported by Wu et al. (2004) and Yoshida et al. (2007), using a similar homogeneization scheme. Nevertheless, FLDs calculated with the MK-VPSC approach fall within the expected behavior. For $0 < \rho \leq 1$, the limit strains move upwards with an increase in the cut-off angle, and the strain limit values never reach those of the random texture (right in Figure 3). Comparison of the two plots in Figure 3 reveals that the behavior observed under the FC framework can be avoided with a more realistic homogeneization scheme like a self-consistent one.

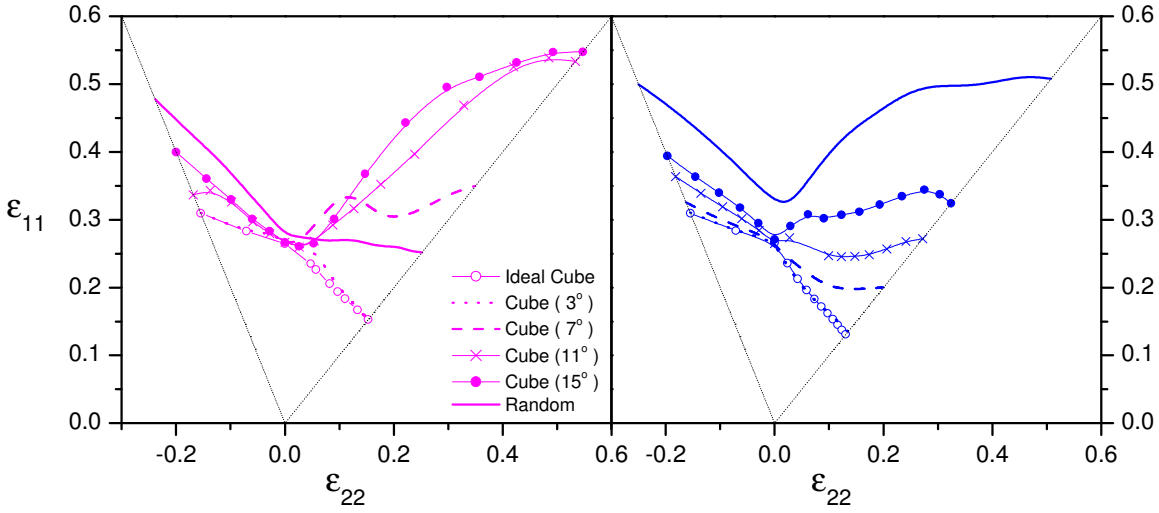

Figure 3: Calculated FLD for MK-FC (left) and MK-VPSC (right) models (m = 0.02, n = 0.24, h_0 = 1218 MPa, τ_0 = 42 MPa).

Previous researchers have demonstrated that yield-surface vertices, anisotropy and material rate sensitivity strongly affect the FLD (Zhou and Neale, 1995; Wu et al., 1997; Wu et al., 1998; Hiwatashi, 1998). Different textures and hence anisotropy evolution produce different shapes and limit strains values. We attribute this behavior to the sharpness of the material yield locus and consequently, to the slip systems selected to accommodate the imposed deformation. To discuss that, the yield-loci calculated using both, FC and VPSC, homogenization schemes are plotted in Figure 4. As expected, for the three presented cases the yield loci calculated with both models are quite different. It can be seen that the curvatures of the VPSC´s yield loci are less sharp than the FC ones, being more pronounced when the initial texture is the random one. This explains the higher limit-strains predicted by the MK-VPSC model as shown in Figure 3. For the other two cube textures (cube 11° and cube 15°) the yield loci are not only sharper but also larger for the FC case. As many other researchers have concluded, all of our simulations confirm that regions of reduced yield-locus curvature correspond to lower FLD values.

Such an analysis can explain the opposite behavior in limit strains reported by previous researchers (Wu et al., 2004; Yoshida et al., 2007), which cannot be understood based only on

initial material textures. In our opinion, the differences in the forming-limit strains are related to material anisotropy and its evolution along the deformation path. This produces an increase or decrease of the FLD profile. Many previous investigations have proven that the VPSC model gives a more realistic description of the anisotropic behavior of polycrystalline materials. We believe that results of the MK-VPSC strategy presented here explain and justify the different effects of the material parameters in a better way.

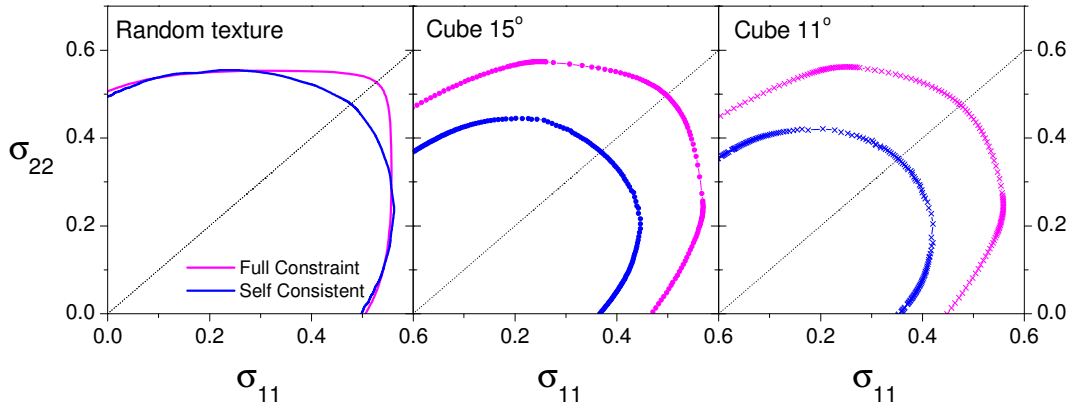

Figure 4: Simulated yield-loci for random (left), cube 15° (center) and cube 11° (right) textures. The equi work-rate surfaces are normalized to the work rate for uniaxial stretching as calculated with the FC model for ρ = 1.

To assess the effect of the cube texture on formability, three more textures are considered in this work. As did Wu et al. (2004), we construct the so-called 25% cube 15°, 50% cube 15° and 75% cube 15°. The corresponding FLDs are shown in Figure 5, where FLDs for a 100% cube 15° and a random texture were included. The results clearly illustrate the differences between the FC (left) and VPSC (right) homogenization schemes, particularly in the biaxial stretching, although the shapes and levels of the FLDs are similar in the negative minor-strain range.

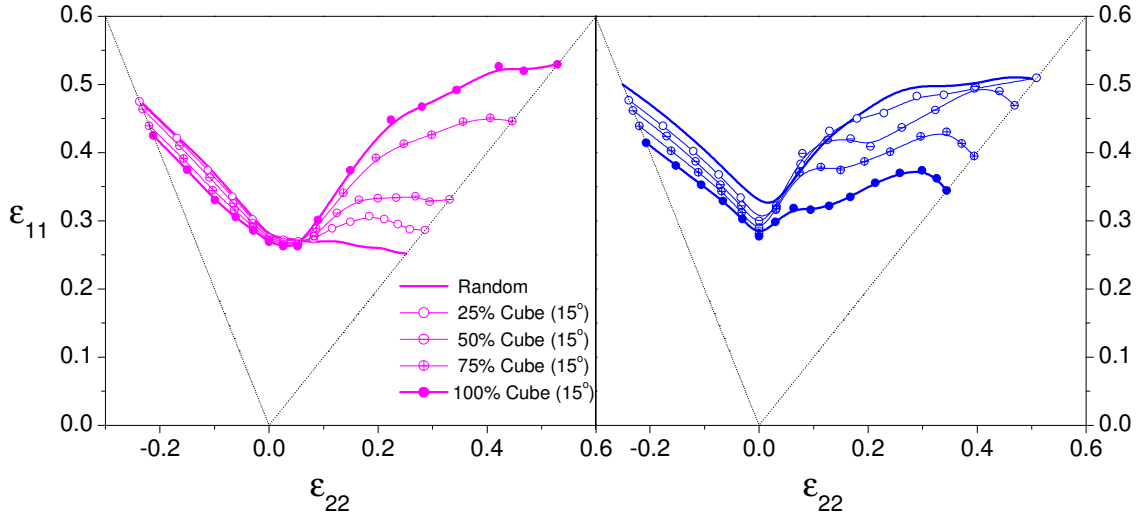

Figure 5: Effect of the cube 15° on the FLDs for MK-FC (left) and MK-VPSC (right) models (m = 0.02, n = 0.24, h_0 = 1218 MPa, τ_0 = 42 MPa).

The corresponding yield-loci after equi-biaxial stretching for the random, 50% cube 15°

and 100% cube 15° are displayed in Figure 6. For VPSC's calculations, the sharpness of the yield locus increases with a decrease of the volume fraction of cube 15°. The opposite behavior is observed for FC's ones, the same situation was reported by Wu et al. (2004).

Although the VPSC model better reproduce the expected results, this assessment requires experimental data to be validated.

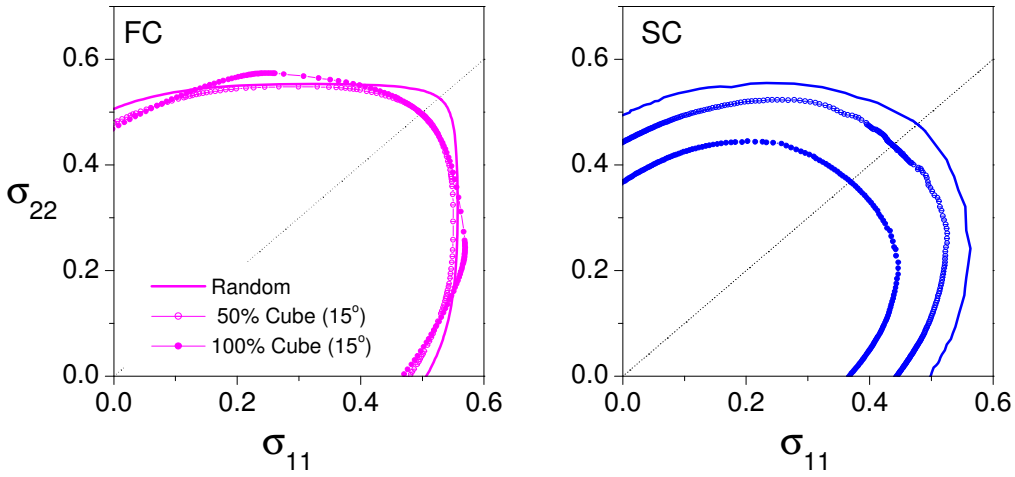

Figure 6: Influence of the cube 15° on the simulated yield loci for FC (left) and VPSC (right) models. The equi work-rate surfaces are normalized to the work rate for uniaxial stretching as calculated with the FC model for ρ=1.

4 CONCLUSIONS

VPSC captures the plastic anisotropy and its evolution showing its capability to better reproduce the material behavior, the anisotropy and its evolution. Notwithstanding, this assessment requires experimental data to be validated. Generalized Taylor-type polycrystal simulations predict higher formability for the cube texture component than that for a random texture in biaxial stretching paths. This unexpected behavior is not observed when a self-consistent homogeneization scheme is employed.

REFERENCES

Barlat, F., and Richmond, O., Prediction of Tricomponent Plane Stress Yield Surfaces and Associated Flow and Failure Behavior of Strongly Textured FCC Polycrystalline Sheets, *Mater. Sci. Technol.*, 95:15–29, 1987.

Hiwatashi, S., Van Bael, A., Van Houtte, P., and Teodosiu, C., Predictions of Forming Limit Strains under Sstrain-Path Changes: Applications of an Anisotropic Model based on Texture and Dislocation Structure, *Int. J. Plasticity* 14:647-669, 1998.

Hutchinson, J.W., and Neale, K.W., Sheet Necking II, Time-Independent Behaviour, in Koistinen D.P. and Wang N.M., Editors, *Mechanics of sheet metal forming*, 127-153, 1978.

Knockaert, R., Chastel, Y., and Massoni, E., Forming Limits Predictions using Rate-Independent Polycrystalline Plasticity, *Int. J. Plasticity* 18:231-247, 2002.

Lebensohn, R.A., and Tomé, C.N., A Self-Consistent Approach for the Simulation of Plastic Deformation and Texture Development of Polycrystals: Application to Zr alloys, *Acta Metall. Mater.* 41:2611–2624, 1993.

Marciniak, Z., and Kuczynski, K., Limit Strains in the Process of Stretch Forming Sheets Metal, *Int. J. Mech. Sci.* 9:609-620, 1967.

Molinari, A., Canova, G.T. and Ahzi, S., A Self-Consistent Approach of the Large Deformation Polycrystal Viscoplasticity, *Acta Metall.* 35:2983–2994, 1987.

Mura, T., *Micromechanics of Defects in Solids*, Dordrecht: Martinus-Nijhoff Publishers, Dordrecht, Netherlands, 1988.

Qiu, Y., Neale, K.W., Makinde, A., and MacEwen, S.R., *Simulations of Materials Processing: Theory, Methods and Applications*, A.A. Balkema, 327-331, 1995.

Signorelli, J.W., Bertinetti, M.A., and Turner, P.A., Predictions of Forming Limit Diagrams using a Rate-Dependent Polycrystal Self-Consistent Plasticity Model, *International Journal of Plasticity,* in press, doi:10.1016/j.ijplas.2008.01.005, 2008.

Viatkina, E.M., Brekelmans, W.A., and Geers, M., A Crystal Plasticity based Estimate for Forming Limit Diagrams from Textural Inhomogeneities, *J. of Mat. Proc. Tech.* 168:211-218, 2005.

Wen, X.Y., Zhai, T., Xiao, C.H., Ningileri, S., Li, Z., Lee, W.B., and Das, S., A Dislocation-Model of Forming Limit Diagrams of FCC Metal Sheet with Combination of Cube and Copper Orientations, *Materials Science and Engineering A* 402:149-157, 2005.

Wu, P.D., Neale, K.W., and Van der Giessen, E., On crystal plasticity FLD analysis. *Proc. R. Soc. Lond.* A 453:1831-1848, 1997.

Wu, P.D., Neale, K.W., Van der Giessen, E., Jain, M., Makinde, A., and MacEwen, S.R., Crystal Plasticity Forming Limit Diagram Analysis of Rolled Aluminum Sheets, *Metallurgical and Materials Transactions* 29A:527- 535, 1998.

Wu, P.D., MacEwen, S.R., Lloyd, D.J., and Neale, K.W., Effect of Cube Texture on Sheet Metal Formability, *Materials Science and Engineering A* 364:182-187, 2004.

Yoshida, K., Ishizaka, T., Kuroda, M., and Ikawa, S., The Effects of Texture on Formability of Aluminum Alloy Sheets, *Acta Materialia* 55:4499-4506, 2007.

Zhou, Y., and Neale, K.W., Predictions of Forming Limit Diagrams using a Rate-Sensitive Crystal Plasticity Model, *Int. J. Mech. Sci.* 37:1-20, 1995.